Molecular Surface Structure of 4,4′,7,7′-Tetrachlorothioindigo Crystal Observed by Atomic Force Microscopy

Kotaro Fukushima*,† and Keigo Gohda‡

Pigments Division, Ciba Specialty Chemicals K. K., Takarazuka 665-8666, Japan, and International Research Laboratories, Ciba-Geigy Japan, Ltd., Takarazuka 665, Japan

Received: September 14, 1998; In Final Form: February 18, 1999

Molecular surface structures of the 4,4′,7,7′-tetrachlorothioindigo crystal, which possessed the excellent photoconduction property, were studied with atomic force microscopy. On the (001) surface, the two-dimensional lattice was slightly enlarged compared with the bulk data, and two kinds of translationally inequivalent molecules could be distinguished in the image. By comparison of the lattice of the monolayer, it was indicated that the molecular planes on the surface were more parallel than those expected from the bulk structure and less parallel than those of the monolayer, and as a result, the HOMO and LUMO that are delocalized in the indigoid part were more likely to be exposed on the surface. On the (110) surface, the two-dimensional lattice expected from the bulk structure almost remained intact on the surface. It was also confirmed on the (110) surface that the molecular planes in two kinds of the stacking columns were nearly parallel to the ⟨110⟩ and that the molecules in one of the stacks were further rearranged in such a way that their molecular longer axes were inclined to the (110) surface. Both the relaxation of the lattice on the (001) surface and the molecular rearrangements on the (110) surface suggested that the intermolecular interactions with stacking neighbors along the *c*-axis strongly predominated over the surface of the tetrachlorothioindigo crystal.

1. Introduction

So far many studies were devoted to identifying the photoconduction process of organic crystals, such as anthracene,[1,2] azos,[3] perylenes,[4] and phthalocyanines.[5] They were mainly aimed at application as charge generation material (CGM) of electrophotographic photoreceptor.[6] Basically, the photoconduction process of the photoreceptor strongly depends on the crystal structure of the organic CGMs, i.e., the molecular arrangement in the crystal, and thus the effects of the crystal structures on the photoconduction have been intensively studied in this field. In our group, the relationship between crystal structures and optical properties was studied using 1,4-dithioketo-3,6-diphenyl-pyrrolo[3,4-*c*]pyrrole (DTPP), which possessed an excellent property as CGM for laser beam printer use.[7]

Moreover, it is quite clear that the photoconduction process of the conventional dual layered photoreceptor is also influenced by the surface/interface structure, especially between the charge generation layer (CGL), in which CGM crystals are loaded, and the charge transport layer (CTL). Therefore, the entire photoconduction efficiency of the photoreceptor is influenced not only by the carrier generation efficiency in the CGM crystal but also by the carrier injection efficiency at the interface. A few kinds of studies have been already done with microscopic[3] and theoretical[8] characterizations of the interfaces. However, it is still unclear what sorts of events at atomic or molecular level are occurring at the interface.

4,4′7,7′-Tetrachlorothioindigo (TCTI; Figure 1) is one of derivatives in the indigo family that shows excellent color property. In addition to this character, its potential as a CGM was already reported by Wiedemann.[9] We also studied its photocarrier generation process with respect to the molecular arrangement in the crystal lattice.[10] It was confirmed that its electrophotographic property was superior to those of the other derivatives, and that its molecular arrangement and the resultant intermolecular interaction in the TCTI crystal were quite suited to the efficient photocarrier generation.

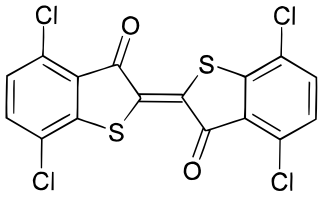

Figure 1. Molecular structure of TCTI.

In this study, we have investigated the molecular surface structures of the TCTI crystal by means of atomic force microscopy (AFM), which enables us to directly observe the surface of organic solids at molecular level.[11−13] The effect of the molecular arrangement on the surface on the photoconduction is also discussed.

2. Experimental Section

TCTI was synthesized from 2,5-dichlorophenyl-1-thioglycollic acid in chlorosulfonic acid and thionyl chloride, and the obtained material was oxidatively dimerized to TCTI.[14,15] The compound obtained was repeatedly purified by a sublimation method where argon gas was flown in quartz tubes with a suitable temperature gradient. The TCTI crystals with a submillimeter size were grown at about 543 K. The shape of the obtained crystals was nearly tetragonal cylinder.

† Ciba Specialty Chemicals K. K. Present address: Colors Division, Ciba Specialty Chemicals K. K., Takarazuka 665-8666, Japan.

‡ Ciba-Geigy Japan, Ltd. Present address : Research Division, Novartis Phama K. K., P.O. Box 1, Takarazuka 665-8666, Japan.

10.1021/jp983705k CCC: $18.00
Published on Web 04/20/1999

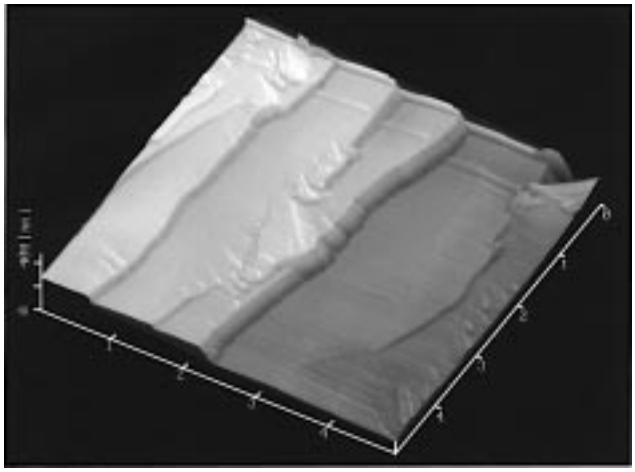

Figure 2. Three-dimensional topographic image of the cleaved (001) surface of the TCTI crystal (5 μm × 5 μm scan). The full scale of the height is 400 nm.

The crystal data of the bulk TCTI structure were monoclinic, $P2_1/a$, $a = 1.3090(4)$, $b = 1.5368(5)$, and $c = 0.3799(1)$ nm, and $\beta = 91.173°$.[10] The molecules form a stacking column along the *c*-axis, which corresponds to the direction of the cylinder.

The crystals were fixed on glass plates for the AFM imaging using epoxy resin (Araldite Rapid, Ciba Specialty Chemicals). For the imaging of the plane normal to the cylinder axis, the crystal was cleaved with a razor blade in advance. All of the images were taken on an SPI 3700 system (Seiko Instruments Ltd.) with repulsive forces on the order of 10^{-9} N at ambient conditions. To minimize the damage of the surface during the scanning, relatively soft Si_3N_4 tips were used whose spring constants were 0.09 and 0.02 N/m and optimum applied forces between the tips and the sample surfaces were selected with constant force mode. Topographic and frictional images were simultaneously taken by a laser detector divided into four parts. Two-dimensional fast Fourier transformation (FFT) was also used for better interpretation of the images. The calibration of the length scale was carried out with atomic scale imaging of mica under the same condition with the imaging of the sample.

For graphic representation of the molecular surface structure of TCTI, a molecular modeling package, MacroModel (Columbia University), was employed.

3. Results and Discussion

3.1. Surface Structure of the Cleaved Plane. Figure 2 shows the AFM image of a cleaved TCTI crystal normal to the cylinder axis, which corresponds to the *c*-axis, with a 5 μm × 5 μm scan. It is seen that the step structures with huge terraces (around 1 μm in width) are formed on this surface. It seems that these terraces correspond to a (001) surface of the TCTI crystal.

When one of the terraces was observed at the higher magnification (20 × 20 nm scan), the two-dimensional lattice could be recognized on the surface (Figure 3). The lattice is a rectangle, and its cell constant is 1.47 ± 0.12 nm × 1.54 ± 0.12 nm. Compared with the dimension of the bulk structure, i.e., $a = 1.31$ nm and $b = 1.54$ nm, the cell constant of the surface is slightly elongated, when deviation of the measurement is taken into account. This is presumably due to a surface relaxation parallel to the surface.

In the TCTI bulk structure, planar TCTI molecules are arranged in such a way that the molecules A (cornered position of the lattice) and the molecule B (centered position) are located normal to each other (Figure 4a), and their molecular planes

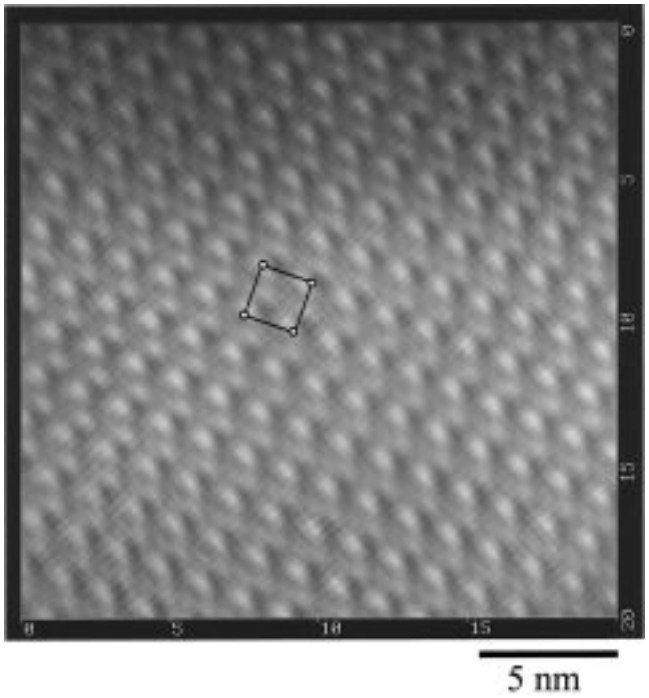

Figure 3. Frictional image of the cleaved (001) surface. The filtering of the image was performed by using 2D-FFT. The square indicated in the image represents a unit cell of the surface structure.

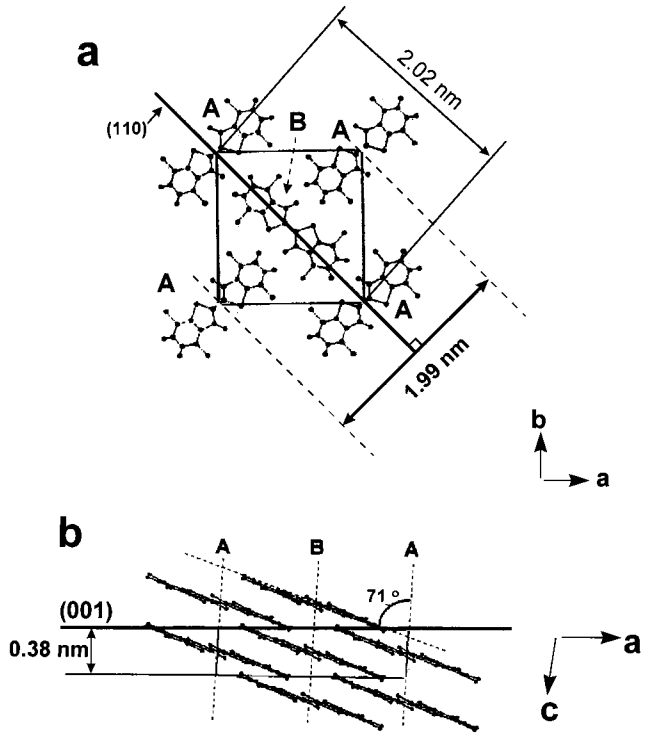

Figure 4. Molecular arrangement of TCTI in the bulk drawn with (a) *a*−*b* projection, (001), and (b) *a*−*c* projection, (010). The (110) surface is also drawn by a line in (a). The angle between the molecular stacks (*c*-axis) and TCTI molecule is indicated as 71° in (b).

are both inclined to the (001) whose slip angle to the *c*-axis is around 71° (Figure 4b). The molecular corrugations on the (001) surface could be seen in the frictional image at the higher magnification (Figure 5a). In the FFT processed image (Figure 5b), the details of the surface structure are clearly seen with the two-dimensional lattice, i.e., diffused bright areas and bright spots are seen around the corner of the lattice and at the center of the lattice, respectively. These two types of contrasts in the

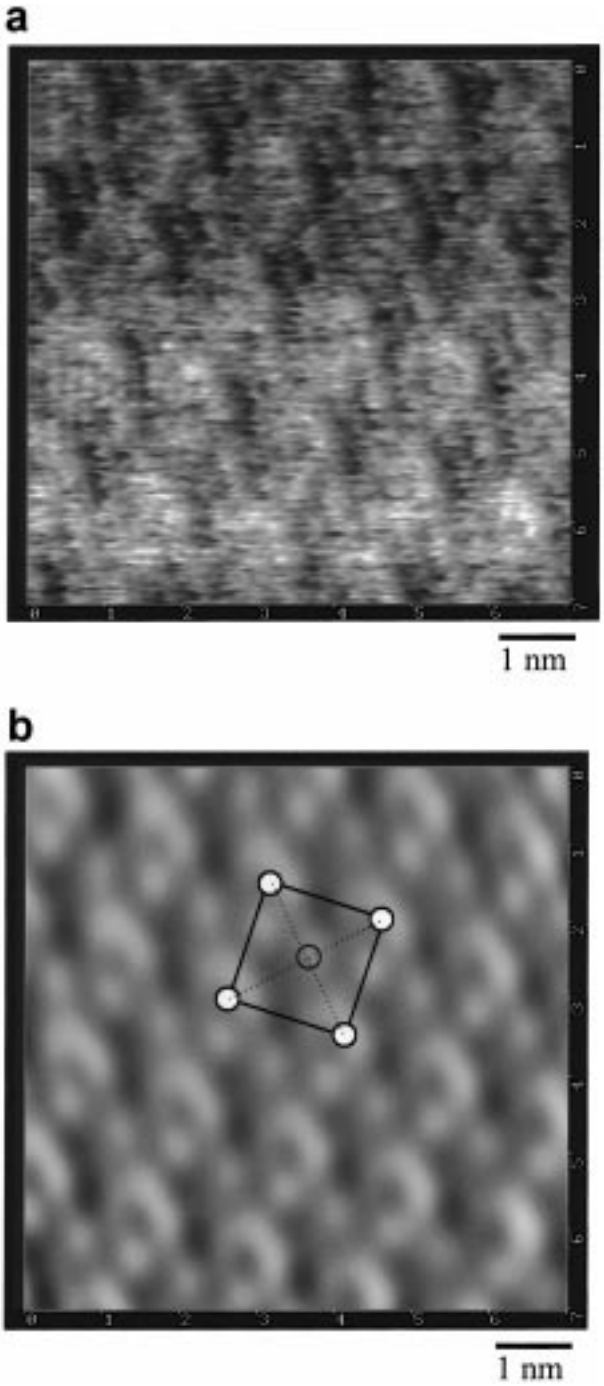

Figure 5. (a) Nonfiltered and (b) 2D-FFT filtered frictional images of the (001) surface of the TCTI crystal with a higher magnification.

AFM image may correspond to the two kinds of molecules in the bulk structure, i.e., the molecule A and B in Figure 4. Then, it is considered that the cornered and centered molecules in the bulk structure are visibly differentiated on the surface.

Recently, Petersen et al. reported by use of scanning tunneling microscope (STM) that a monolayer of TCTI formed the two-dimensional lattice on the crystalline substrates at an ambient condition, in which the molecular planes of TCTI were parallel to the substrates with a tetragonal lattice of $a = 1.51 \pm 0.05$ nm, $b = 1.55 \pm 0.05$ nm irrespective of the kind of substrates, and that the molecular arrangement of the monolayer was quite similar to that of the (001) in the bulk structure where the cornered molecule and centered molecules in the lattice are arranged normal to each other.[16] Furthermore, they estimated the area per molecule as 1.2 nm.^{2} In our experimental result,

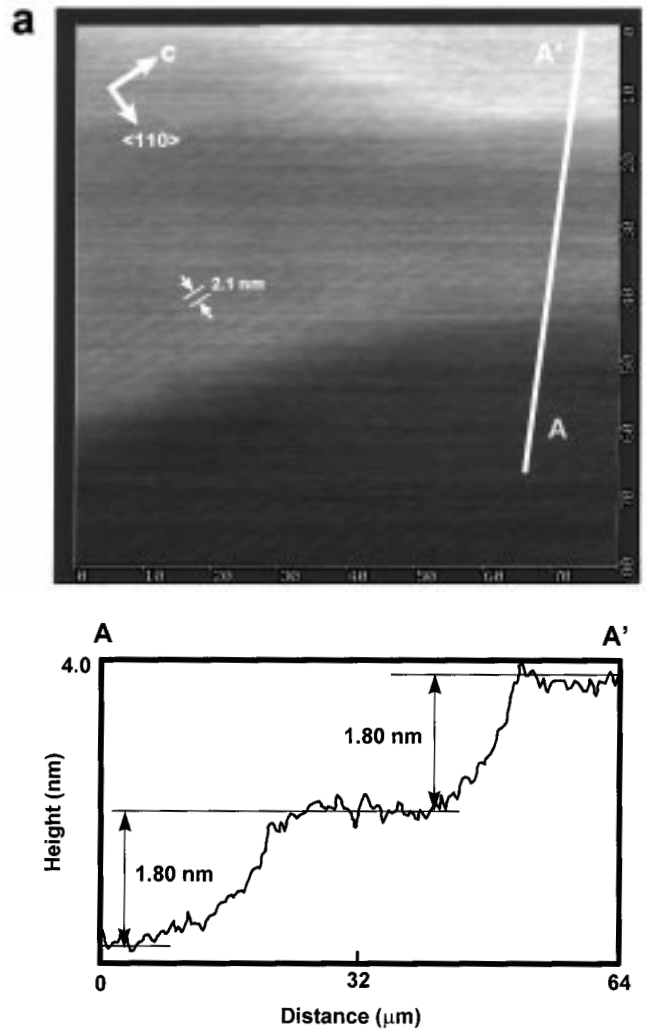

Figure 6. (a) Topographic image of the side plane of a tetragonal cylinder crystal (80 μm $\times$ 80 μm scan). (b) Cross section profile as indicated by the line in (a).

the area per molecule of the (001) surface is calculated as 1.1 nm.^{2} This value is greater than 1.0 nm^2 estimated from the bulk data and smaller than that for the monolayer. Therefore, it is expected that, on the (001) surface, the molecular plane of TCTI is more parallel to the surface than those expected from the bulk structure and less parallel than those of the monolayer and that this molecular motion induces the relaxation of the lattice.

From the viewpoint of the photoconduction of the TCTI crystal, the $\pi-\pi$ stacks along the *c*-axis play a major role.[10] Because the π-electrons in the HOMO and LUMO of the TCTI molecule are delocalized in the cross-conjugated part of the TCTI molecule, i.e., indigoid part, the electrons/holes easily migrate to the stacking neighbor through the effective overlaps of HOMOs and LUMOs between them. Correspondingly, the intermolecular $\pi-\pi$ interactions between the topmost molecules and underlying molecules is expected to dominate the molecular arrangement on the (001) surface. The HOMO/LUMO are likely to be exposed to the surface more than that expected from the bulk structure due to the surface relaxation of the lattice. Then, this structure of the (001) surface may be also suitable for an additional process, i.e., an injection of the carrier to the charge transport material (CTM).

3.2. Surface Structure of the Noncleaved Plane. Figure 6a shows the surface structure of one of the four singular planes that is parallel to the cylinder axis (*c*-axis). The periodicity of the lattice in Figure 6a is 2.10 ± 0.16 nm. This value is identical

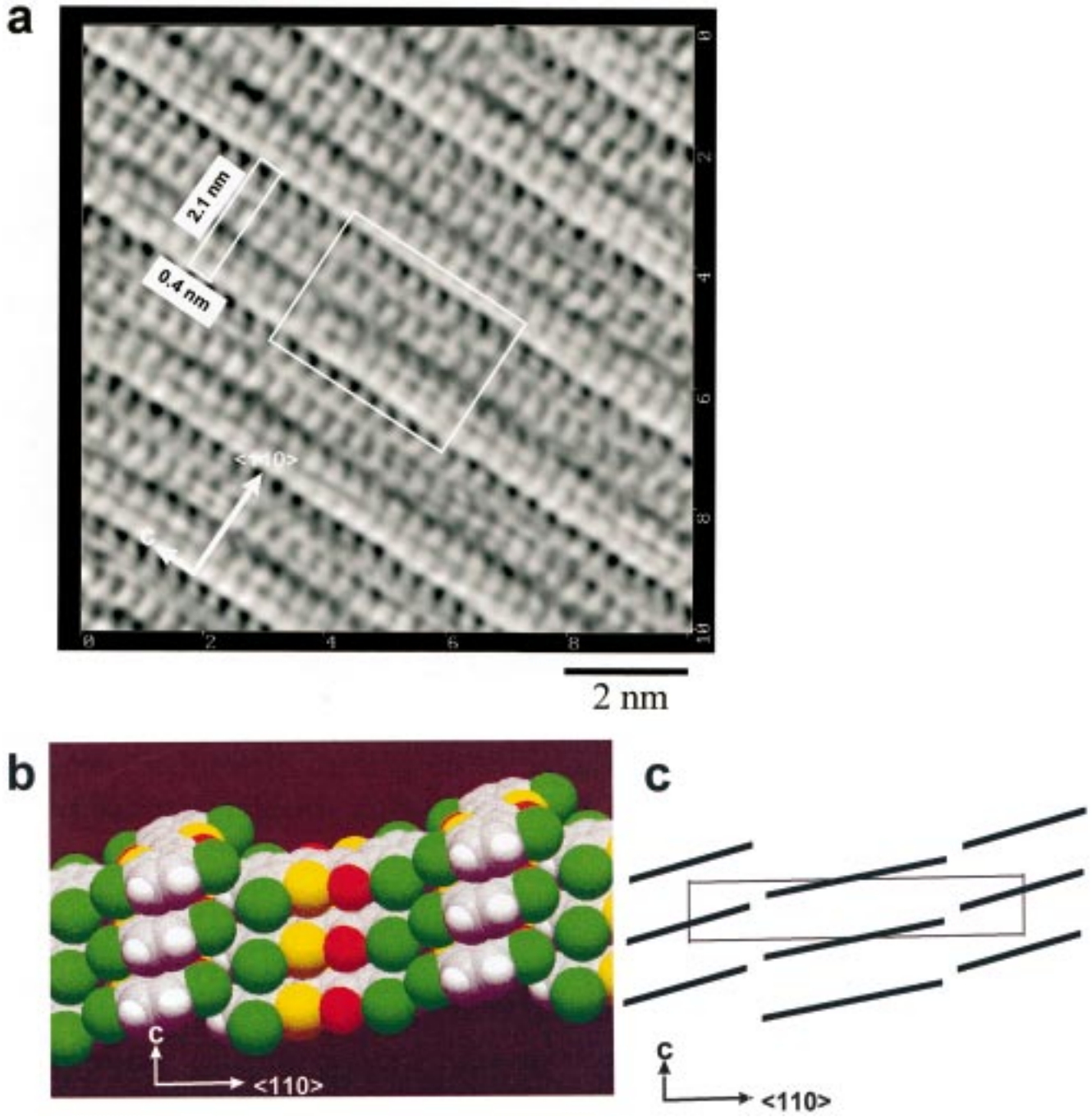

Figure 7. (a) Frictional image of the (110) surface after the 2D-FFT filtration. A rectangular area corresponding to the averaged cross section along ⟨110⟩ is presented in Figure 8a. (b) Graphic representation of the (110) surface expected from the bulk data. The molecular corrugations are represented with van der Waals radii. (c) Schematic representation of the surface corrugation on the (110) surface expected from the bulk structure.

to 2.02 nm, which is expected to occur on the (110) surface structure based on the bulk data within the experimental error (Figure 4a). The cross section of the AFM image shows the step structure whose height is 1.80 ± 0.20 nm (Figure 6b). This value is also close to 1.99 nm, which is expected to occur as a molecular step of the (110) based on the bulk structure (Figure 4a). At the higher magnification, a two-dimensional lattice with molecular corrugations is obtained, as shown in Figure 7a. The periodicity along the *c*-axis on the surface is 0.40 ± 0.03 nm, which is also equal to 0.38 nm of the cell constant along the *c*-axis within the experimental error. Thus it seems that the surface observed should be one of the {110} surfaces.

Figure 7b shows the molecular arrangement on the (110) expected from the bulk structure. In this arrangement, the image on the surface should show the line-shaped corrugations corresponding to the planar TCTI molecules, and the lines should be inclined to the major axis of the lattice, as shown in Figure 7c. However, the result shows that line-shaped corrugations on the (110) surface are almost normal to the *c*-axis (Figure 7a). This means that a rearrangement of the molecule occurs on the (110) surface with cooperative motion of the stacking molecules. It is expected that the strong intermolecular $\pi-\pi$ interaction between stacking neighbors along the *c*-axis are dominantly operated to determine the molecular arrangement on the (110) surface. Also on the (001) surface, the $\pi-\pi$ interactions along the stacks may play a major role for the rearrangement of the molecule, as mentioned above.

Figure 8a shows the cross section profile along the ⟨110⟩. It

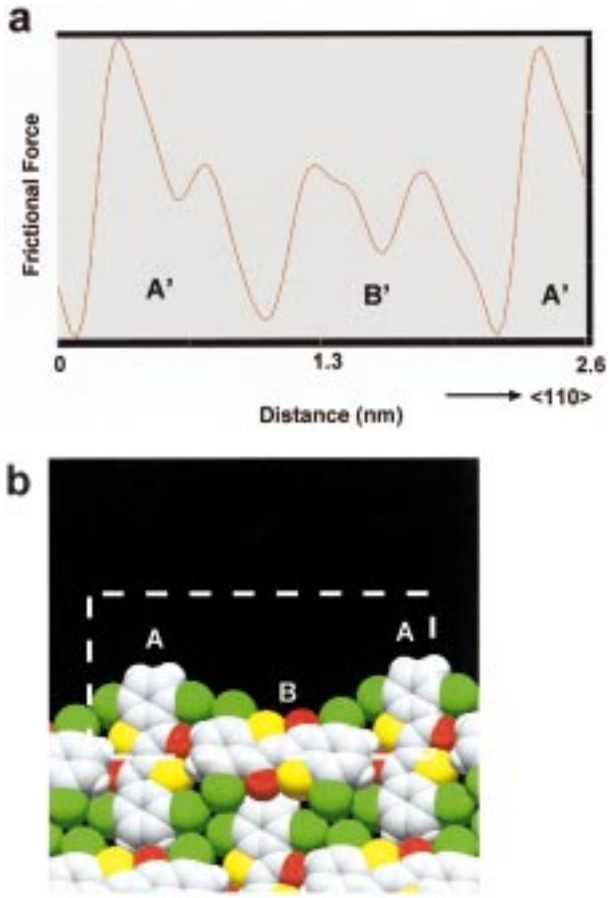

Figure 8. (a) Averaged cross section along ⟨110⟩ on the (110) surface as indicated by the rectangular area in Figure 7a. (b) Graphic representation of the cross section of the (110) surface expected from the bulk data. The molecular corrugations are represented with van der Waals radii. Molecules A and B correspond to those in Figure 4a.

shows the averaged data obtained over the area indicated with the rectangle in Figure 7a. Two different molecular corrugations can be seen, i.e., stack A′ and stack B′, in which two kinds of inequivalent molecules are included, respectively. This may correspond to the projections of molecule A and molecule B in Figure 4a. Stack B′ on the surface shows the two broad peaks with almost equal height, each of which might correspond to half of the TCTI molecules (Figure 8b). It seems that the molecular longer axes in this stack are parallel to the surface, as expected. In the case of stack A′, it possesses two peaks with different heights (Figure 8a). The molecular longer axis of molecule A is located almost normal to the surface and its cross section must reveal the correspondingly symmetrical one in the bulk structure (Figure 8b). Therefore, the molecules in stack A′ should be further rearranged in such a way that the molecular longer axis is inclined to the (110) surface.

Taking into account the closed-packed structure in the bulk, it might be difficult to keep the cell dimension intact on the surface with the molecular rearrangement. Therefore, the lattice on the (110) surface may include the relaxation, although the difference from the lattice in the bulk was not distinguished in the result.

4. Conclusions

The characteristic planes of the TCTI crystals, i.e., (001) and (110), were investigated using AFM. The results indicated that the molecular arrangements on both planes slightly differed from those expected from the bulk structure. The arrangement on the (001) surface seemed to be constrained by the intermolecular interactions with underlying molecules, while on the (110) surface the molecular rearrangement was governed with cooperative motions of the stacking molecules. A characteristic strong intermolecular interaction between the stacking TCTI molecules was already confirmed with molecular conformational analysis compared with those of the other thioindigo derivatives.[10] Therefore, it is concluded that the strong molecular interactions between stacking neighbors in the bulk strongly affected the formation of the molecular surface structures. Then, these interactions substantially lead to the excellent photoconduction property of the TCTI crystal. A comparative AFM study using other derivatives will provide supporting evidence for the result in this study. Furthermore, this kind of approach will be useful for experimental evaluation of the anisotropic intermolecular interactions which substantially exist in organic crystals.

References and Notes

(1) Chance, R. R.; Braun, C. L. *J. Phys. Chem*. **1976**, *9* (1), 3573.
(2) Sebastian, L.; Weiser, G.; Peter, G.; Bässler, H. *Chem. Phys*. **1983**, *75*, 103.
(3) Niimi, T.; Umeda, M. *J. Appl. Phys*. **1994**, *76* (2), 1269.
(4) Popovic, Z. D.; Loutfy, R. O.; Hor, A.-M. *Can. J. Chem.* **1985**, *63*, 134.
(5) Simon, J.; Andre, J.-J. *Molecular Semiconductor*; Springer-Verlag: Berlin, 1984; Chapter 3.
(6) Shattuck, M. D.; Vahtra, U. U. S. Patent 3,484.237, 1969.
(7) Arita, M.; Fukushima, K.; Homma, S.; Kura, H.; Yamamoto, H.; Okamura, M. *J. Appl. Phys*. **1991**, *70*, 4065.
(8) Pacansky, J.; Waltman, R. J.; Berry, R. *J. Chem. Mater*. **1995**, *7* (5), 840.
(9) Wiedemann, W. *Second International Conference of Electrophotography* **1974**, 224.
(10) Fukushima, K.; Nakatsu, K.; Takahashi, R.; Yamamoto, H.; Gohda, K.; Homma, S. *J. Phys. Chem. B* **1998**, *102* (31) 5985.
(11) Gould, S.; Marti, O,; Drake, B.; Hellemans, L.; Bracker, C. E.; Hansma, P. K.; Keder, N. L.; Eddy, M. M.; Stucky, G. D. *Nature* **1988**, *332*, 332.
(12) Overney, R. M.; Howald, L.; Frommer, J.; Meyer, E.; Brodbeck, D.; Güntherodt, H.-J. *Ultramicroscopy* **1992**, *42*−*44*, 983.
(13) Nakamura, M.; Tokumoto, H. *Surf. Sci*. **1997**, *377*−*379*, 85.
(14) Shiha, A. K.; Bose, A. J. *Indian Chem. Soc*. **1977**, *LIV*, 428.
(15) Schuetze, Detlef Ingo. Ger. Offen. DE 3,117,056, 1991.
(16) Peterson, J.; Strohmaier, R.; Gompf, B.; Eisenmenger, W. *Surf. Sci*. **1997**, *389*, 329.